

Dihydrazone of dialdehyde starch and its metal complexes

Andrzej Para*, Stanisława Karolczyk-Kostuch, Maciej Fiedorowicz

Department of Chemistry, University of Agriculture, Al. Mickiewicza 21, 31-120 Kraków, Poland

Received 12 May 2003; revised 29 December 2003; accepted 2 February 2004

Available online 10 March 2004

Abstract

Dialdehyde starch (32%) from periodate oxidized potato starch was converted into its dihydrazone (DASHZ). It was considered as a potential trap of heavy metals from sewage and in soil. The dihydrazone (DASHZ) coordinated to Ca, Cd, Co (II), Cu (II), Fe (II), Mg, Mn (II), Ni (II), Pb (II), and Zn ions. The nitrogen atoms of the C=N moiety in dihydrazone as well as the oxygen atom of the former pyranose ring were the coordination sites. Metal ions were chelated to a different extent. One mole of a metal ion could coordinate with 3 [Cu(II)] to 50 [Mn(II)] mole of the DASHZ units. Similarly, as DASHZ, the metal complexes decomposed thermally in four steps but the rates of decomposition of the ligand and chelates in relevant steps were different. Except the complex with Mg, these rates for complexes were lower. © 2004 Elsevier Ltd. All rights reserved.

Keywords: Dialdehyde starch; Dialdehyde starch dihydrazone; Metal complexes

1. Introduction

Several hydrazones have exhibited specific pharmacological activity designing them to the role of antineoplastic, antiviral, and anti-inflammatory agents (Constable, Khan, Lewis, Liptrot, & Raithby, 1985; Giordano, Palenik, Palenik, & Sullivan, 1979; Latha, Vaidya, Keshavayya, & Vagdevi, 2001; Rakha, Ibrahim, Abdallah, & Hassanian, 1996; Singh, Singh, & Singh, 2001). It has also been shown that hydrazones coordinated to metal ions increased and even changed the kind of their biological activity. Several metal complexes of hydrazones have been used as antitumour agents (Johnson, Murphy, Rose, Goodwin, & Pickart, 1982; Yang, Yang, Li, & Yu, 2000). Transition metal complexes of hydrazone compounds have also been screened for their bactericidal activity (Agarwal, Jain, & Chand, 2002; Nawar & Hosny, 2000; Tsukamoto, Sato, Tanaka, & Yanai, 1997).

It is known (Saripinar et al., 1996; Von Wagner & Winkelmann, 1972) that thiosemicarbazones of aromatic and heteroaromatic aldehyde, but not thiosemicarbazones of aliphatic aldehydes, exhibited tuberculostatic activity. Unexpectedly, dithiosemicarbazone of dialdehyde starch (DAS), which was an aliphatic aldehyde, and its metal complexes (Para, Klisiewicz-Pańszczyk, & Jurek, 2001)

showed unusually potent tuberculostatic activity. This result induced, presented in this paper, preparation of unknown starch dialdehyde dihydrazone (DASHZ) and its complexes with the Ca, Cd, Co(II), Cu(II), Fe(II), Mg, Mn(II), Ni(II), Pb(II), and Zn ions for further biological screenings.

Apart from their potential biological activity, dihydrazone of DAS might be considered as a biodegradable trap for heavy metal ions from sewage. Similarly as both DAS dithiosemicarbazone and disemicarbazone (Para & Ropek, 2000; Ropek & Para, 2002) they could offer an immobilization of the heavy metal ions in the soil in various periods of the crop production. DASHZ could improve existence conditions of beneficial soil microorganisms such as entomopathogenic nematodes and fungi within their seasonal activity.

2. Experimental part

DAS oxidized in 32% was prepared from potato starch (manufactured by PPZ Trzemeszno, Poland) in the periodate oxidation with electrochemical recovery of the oxidant according to Para, Karolczyk-Kostuch, Hajdon, and Tomasiak (2000). Water solubility at 25 °C of so prepared DAS reached 2.2%. HPLC-determined molecular weight profile was as follows: <1000 13, 1000–40,000 69, and 40 000–250,000 – 18% of the total.

* Corresponding author. Tel.: +4812-662-41-39; fax: +4812-662-43-45.
E-mail address: rrpara@cyf-kr.edu.pl (A. Para).

Dialdehyde starch dihydrazone (DASHZ) was prepared according to Para et al. (2000) with hydrazine sulfate, reagent grade (POCH Gliwice, Poland).

The salts used: $\text{CaCl}_2 \cdot 2\text{H}_2\text{O}$, $\text{CdCl}_2 \cdot 2.5\text{H}_2\text{O}$, CoCl_2 , $\text{CuCl}_2 \cdot 2\text{H}_2\text{O}$, $\text{FeCl}_2 \cdot 4\text{H}_2\text{O}$, $\text{MgCl}_2 \cdot 6\text{H}_2\text{O}$, $\text{MnCl}_2 \cdot 4\text{H}_2\text{O}$, NiCl_2 , $\text{Pb}(\text{NO}_3)_2$ and ZnCl_2 were of analytical grade. They were purchased from POCH, Gliwice, Poland.

2.1. Average molecular weight of DAS

High pressure size exclusion chromatography system consisted of Shimadzu LC10A pump (Shimadzu Japan), Rheodyne model 7725i injector (Rheodyne, USA), column TSKgel GMPWXL (7.8×30 mm, TosoHaas, Japan) and differential refractive index detector Merck LaChrom L-7490 (Merck, Germany). Mobile phase was 0.15 M NaNO_3 , with 0.02% NaN_3 pumped with flow rate $0.5 \text{ cm}^3/\text{min}$. Injector, column and detector temperature was maintained at 25°C . Starch derivatives were dissolved in mobile phase ($20 \text{ mg}/\text{cm}^3$) and $100 \mu\text{l}$ volumes were injected on the column. Column was calibrated with set of 10 dextran standards (Polygen, Denmark) with M_w ranging from 1080 to 401300. Data were collected and analyzed with Merck D-7000HSM software.

2.2. Preparation of complexes

DASHZ (2 g) with 0.004 mole hydrazone moieties was suspended in 0.5 M aqueous solution (10 cm^3) of a given metal salt and agitated gently for 3 h. Then the suspension was filtered under reduced pressure using the chemistry diaphragm pump MZ 2C, (Vacuubrand GmbH and Co. KG, Wertheim, Germany) and washed on the MN 640 m filter (Macherey-Nagel GmbH and Co. KG, Düren, Germany) with distilled water ($3 \times 20 \text{ cm}^3$) under a medium filtration speed. The solid was dried in a convective dryer at 100°C to the constant weight. The reaction yield was calculated in respect to the initial weight of the ligand.

2.3. Elemental analysis

Nitrogen content was estimated using the Dumas semi-micro combustion analysis (Bobrański, 1956). The metal content was determined with inductively coupled plasma-atomic emission spectrometer ICP-AES, JY 238 ULTRACE JOBIN-YVON, (Longjumeau, France).

2.4. Solubility in water

Solubility was estimated according to Richter, Augustat, and Schierbaum (1968). Complexes (0.1 g) were dissolved in distilled water (8 cm^3) and agitated for 30 min in a water bath at 25°C then centrifuged (5000 rpm for 10 min). Resulting transparent solution (5 cm^3) was transferred to the weighing dish of constant weight and evaporated and dried in a convective dryer at 120°C to a constant weight.

2.5. Ultraviolet (UV) absorption spectra

The spectra of 2.8×10^{-3} M aqueous solutions were recorded in 10 mm quartz cells using the UV–VIS Scanning Spectrophotometer, Shimadzu UV-2101 PC (Kyoto, Japan).

2.6. Fourier transformation infrared (FTIR) spectra

The FTIR spectra in KBr discs were recorded in the 650 – 4000 cm^{-1} region with BIO-RAD, STS-60 V spectrophotometer (Cambridge, USA).

2.7. Raman spectra

Raman spectra were registered using a Bio-Rad FT Raman spectrometer (Cambridge, USA) with diode Spectra-Physics Nd: YAG laser (the 1064 nm line).

2.8. Electron paramagnetic resonance (EPR) spectra

Experiments were carried out on X-band Bruker ESP-500 spectrometer (Karlsruhe, Germany) with the 100 KHz field modulation. The spectra were recorded at room temperature and at 77 K. EPR parameters were found by means of simulation with involvement of modified SIM 14 program (Lozos & Hoffman, 1974).

2.9. Thermal analysis

Samples (0.1 g) were heated from 21 to 500°C in corundum crucibles in the open at the $10^\circ\text{C}/\text{min}$ rate of temperature increase. Corundum particles having $\phi = 8 \mu\text{m}$ were taken as the standard. Analysis was performed with a computerised Paulik-Paulik-Erdey Q-1500-D (Budapest, Hungary) apparatus.

2.10. Magnetic susceptibility

The magnetic dc-susceptibility measurements were carried out using a commercial Quantum Design SQUID magnetometer (San Diego, USA) in the magnetic field of 2 Tesla and in temperature range from 10 to 300 K. Effective magnetic moments of the metal ions were estimated from the slope of the inverse susceptibility, after taking into account diamagnetic background.

3. Results and discussion

The yield of the complex formation, solubility of complexes, and their elemental analysis are presented in Table 1.

The yield of complexation of DASHZ (Fig. 1) with metal ions was high (82–96%).

Water-solubility of the most of the DASHZ complexes was comparable with solubility of the ligand and only

Table 1
Characteristics of starch dialdehyde dihydrazone and its metal complexes

Central metal atom	Colour	Reaction yield ^a (%)	Water solubility (%)	Elemental analysis			
				Nitrogen (%)		Metal ions	
				Calcd.	Found	$\frac{g \times 10^{-3}}{1gDASHZ}$	$\frac{X^b}{mol M}$
None	Yellow		1.2	10.44	10.95		
Ca	Yellow	82	1.3	10.37	10.13	6.80	12
Cd	Dark yellow	94	4.8	10.19	9.75	24.50	9
Co(II)	Light brown	89	1.8	10.37	9.93	6.25	18
Cu(II)	Dark brown	87	4.5	10.01	9.24	43.15	3
Fe(II)	Brown yellow	92	1.0	10.38	10.48	5.70	20
Mg	Yellow	90	1.0	10.43	10.18	1.12	40
Mn(II)	Yellow	88	2.1	10.42	10.10	2.20	50
Ni(II)	Brown	92	1.8	10.35	9.58	8.80	13
Pb(II)	Orange yellow	96	5.0	10.07	10.14	36.30	12
Zn	Dark yellow	93	1.9	10.38	9.63	5.90	22

^a Calculated on DASHZ.

^b The number of moles of DASHZ units.

coordination to Cd(II), Cu(II), and Pb(II) provided about four times higher solubility. The level of ions coordinated to DASHZ varied within the range of 3–50 moles of the dihydrazone unit on 1 mole of the metal. Analysis for the nitrogen content usually fitted calculated values within the range of the 0.5% error. For the Cu(II), Ni(II) and Zn(II) complexes this error was within the 0.8% limit.

Table 2 presents the UV and Raman spectral characteristics of the ligand and its metal complexes.

In the UV spectrum of DASHZ two absorption bands at 193.6 nm ($A = 1.913$) and 278 nm ($A = 1.643$) could be observed. Coordination to metal had practically no influence on the position and intensity of the first spectral band. Also, except for the Cu(II) complex (285.6 nm), the position of the second band representing the local absorption in the $-\text{CH}=\text{N}-\text{NH}_2$ chromophore was insensitive to coordination. A decrease in absorbance was common in the spectra of all complexes. The band intensities in the spectra of the Co(II) (0.984) and Cu(II) (0.880) complexes were the lowest. The decrease in the intensity was paralleled by an increase in the number of the central metal atoms in complexes.

In the IR spectrum of the DAS and its derivatives an intense band at 1637 cm^{-1} assigned to water was present. It covered the $\nu(\text{C}=\text{N})$ stretching vibrations in DASHZ. Therefore, the Raman spectra in the region of $4000\text{--}200\text{ cm}^{-1}$ were recorded instead.

The Raman spectrum of DAS exhibited an intense band at 1732 cm^{-1} assigned to the $\nu(\text{C}=\text{O})$ stretching vibration in the aldehyde carbonyl group. This band vanished in the spectrum of DASHZ confirming formation of dihydrazone. In a consequence, the band at 1585 cm^{-1} attributed to the $\nu(\text{C}=\text{N})$ stretching could be observed. This band was fairly sensitive to coordination. Especially in the spectrum of the Cu(II) complex it moved to lower frequency as a result of reduced electron density at the nitrogen atom caused by coordination to a metal cation (Nawar & Hosny, 2000;

Radecka-Paryzek & Gdaniec, 1997). In the spectrum of free ligand (Fig. 2), there was a shoulder on the red side- slope of this band suggesting an overlap of two bands. It might reflect a non-equivalence of two hydrazone groups in DASHZ. In the spectra of DASHZ metal complexes, the shoulder turned into a fairly well separated band in the region of $1555\text{--}1561\text{ cm}^{-1}$ depending on the central metal ion in the complex (Table 2). The spectrum of the Cu(II) complex was exceptional because of a larger shift of that band to lower frequency (1500 cm^{-1}). Changes in the ratio of the $\nu(\text{C}=\text{N I})-\nu(\text{C}=\text{N II})$ band intensity could suggest the participation of only one hydrazone group in the coordination.

In the region above 1450 cm^{-1} , the spectra of complexes contained bands assigned to vibrations in the polysaccharide backbone. These bands could cover spectral changes resulting from coordination.

The EPR spectrum of the Cu(II) complex recorded at room temperature and at -196°C contained two peaks (Table 3). The weak signal at low field independently of the measurement temperature had $g = 2.470$. It was interpreted as g_{\parallel} . The g -factor of the strong signal at high field (g_{\perp}) slightly varied between 2.034 and 2.033 at room temperature and -196°C , respectively. The value of $g_{\parallel} > 2.3$

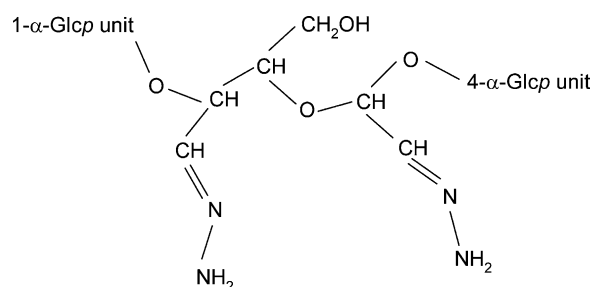


Fig. 1. Potential structure of dialdehyde starch dihydrazone.

Table 2
UV and Raman spectra of dialdehyde starch dihydrazone and its metal complexes

Central metal atom	UV ^a				Raman shift ^b	
	λ_{\max} I [nm]	A	λ_{\max} II [nm]	A	$\nu(\text{C=N I}) [\text{cm}^{-1}]$	$\nu(\text{C=N II}) [\text{cm}^{-1}]$
None	193.6	1.913	278.0	1.643	1586	
Ca	192.2	1.797	276.8	1.548	1588	1558
Cd	193.4	1.819	276.8	1.536	1586	1555
Co(II)	191.8	1.816	276.8	0.984	1586	1559
Cu(II)	193.0	1.820	285.6	0.880	1570	1500
Fe(II)	192.2	1.876	279.2	1.498	1584	1557
Mg	193.6	1.890	277.6	1.637	1586	1557
Mn(II)	193.0	1.898	278.2	1.640	1586	1556
Ni(II)	193.4	1.804	277.6	1.236	1587	1561
Pb(II)	191.6	1.783	278.2	1.494	1588	1557
Zn	193.6	1.808	277.8	1.427	1586	1559

^a A and λ_{\max} denote the absorbance and position of the longest wavelength maxima, respectively.

^b The wavenumbers of the corresponding C=N bands.

indicated the ionic nature of the complex (Shakir & Varkey, 1994). The G parameter obtained from the expression $G = (g_{\parallel} - 2)/(g_{\perp} - 2)$ exceeded 4, suggesting that exchange interactions between Cu(II) centers in the solid state were negligible (Narang, Pardey, & Singh, 1994).

Magnetic moments were measured indirectly. The magnetic susceptibility of a material was measured from which, magnetic moments of the paramagnetic ion or atom therein could be calculated.

The magnetic susceptibilities for the Co(II) and Cu(II) complexes at different temperatures successfully fitted the Curie-Weiss law (Cotton & Wilkinson, 1962a).

$$\mu = 2,84\sqrt{\kappa_M^{\text{COOR}}(T - \theta)}$$

with μ , κ_M^{COOR} , T , and θ being the magnetic moment (in BM, magneton of Bohr), paramagnetic susceptibility per mole, corrected for the diamagnetism due to closed shells, absolute temperature, and Weiss constant (empirically found), respectively.

The effective magnetic moments were 4.47 and 1.13 BM, respectively (Table 4).

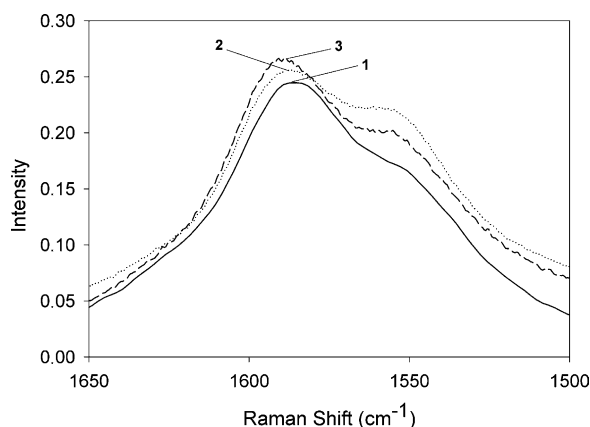


Fig. 2. Raman spectra of: 1. DASHZ (1586 cm^{-1}); 2. Cd(II) complex (1586 cm^{-1} , 1555 cm^{-1}); 3. Pb(II) complex (1588 cm^{-1} , 1557 cm^{-1}).

Reported moments for tetrahedrally coordinated Co(II) varied between 4.1 and 4.9 BM. In this case an inverse relationship between the magnitude of the orbital contribution and the strength of the ligand field was found (Cotton & Wilkinson, 1962b).

The expected range for magnetically diluted Cu(II) complexes extended between 1.7 and 2.2 BM. Several complexes with the magnetic moments below this range indicated antiferromagnetic coupling. Copper used to form a number of compounds with the Cu–Cu distances short enough to provide significant Cu–Cu interactions but in no case these distances corresponded to the Cu–Cu bonds (Cotton & Wilkinson, 1972; Koh et al., 1998). The value of 1.13 BM reflected the polymeric character of the DASHZ-Cu(II) complex.

Frequently, ligands containing the hydrazone moiety and oxygen atoms utilize simultaneously the nitrogen and oxygen atoms as coordination centers for metal ions (Abou Sekkina & Salem, 1997; Li, Wang, Meng, & Zhao, 1999; Nawar & Hosny, 1999; Nawar & Hosny, 2000). The structure presented in Fig. 3 proposed for the complexes of the metal ions and DASHZ followed the same assumption.

The heat of formation per one bond was calculated with HyperChem Pro 6.0 software. The calculations were performed for all possible complex structures derived from the involvement of the nitrogen and oxygen atoms leading to the formation of either five-, six-, and, simultaneously, five- and six-membered rings. The lowest heat of formation (-697.2 kJ/bond) among all calculated

Table 3
EPR spectra of the DASHZ-Cu (II) complex

	g-Factor	
	Room temperature	Liquid nitrogen temperature
Parallel	2470	2470
Perpendicular	2034	2033

Table 4
The effective magnetic moments for the Co(II) and Cu(II) complexes

	Magnetic moment [BM]
Co (II)	4.47
Cu (II)	1.13

structures has that shown in Fig. 3, which seems to be the most stable and dominant species. Little differences in calculated values of heat of formation (of the order of a few kJ) did not preclude other ways of coordination with nitrogen and oxygen atoms, especially, when various metal ions were taken under consideration.

The thermal properties of DASHZ and its metal complexes are presented in Table 3.

DASHZ trapped certain amount of water (6.2%) and such behaviour was typical for polysaccharides. Water content in the complexes was reduced to 2.4–4.7%. After the evolution of water was determined from decrease of the thermogravimetric (TG) curve, the ligand and complexes decomposed in four further stages. First, between 180 and 230 °C the complexes usually lost 15–17% of their weight. Only the weight loss from the Cu(II) and Pb(II) complexes was lower, 12.4 and 13.6%, respectively. In the subsequent stage from 230 to 270 °C all complexes lost 9–10% of their weight and only Cu(II) and Ni(II) complexes lost more of their weight, 12.7 and 11.1%, respectively. Between 270 and 310 °C the weight loss was also between 9 and 10%. Approximately 13% weight loss was typical for the decomposition of the majority of complexes in the fourth step from 310 and 400 °C. The overall weight loss (21–400 °C) for all complexes except the Cu(II) complex was between 50 and 56% and only in the latter case the weight loss reached hardly almost 46%. These values show, that metal ions did not catalyse the thermal decomposition of the complexes, in contrast, these compounds [except Mg(II) complex] are more stable in the temperature range of 21–400 °C than the ligand (Table 5).

The rate of decomposition of the Mg complex in the second stage ($\text{tg } \alpha = -0.71$), this is the next after the water evolution, was higher than that of the pure ligand ($\text{tg } \alpha = -0.66$) (Table 5). The coordination to Ca had no influence on the rate of decomposition in the same stage. It was quite the same as that for the pure ligand ($\text{tg } \alpha = -0.64$) (Table 5). The other complexes decomposed with a lower rate. The slope of the TG line given in

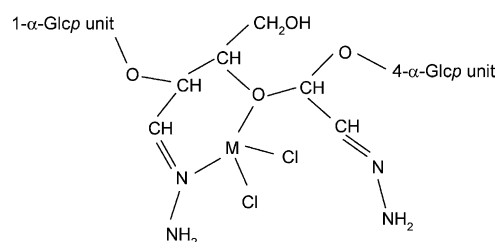


Fig. 3. Potential structure of metal complexes of DASHZ.

Table 5
Thermal analysis (TG, DTG) of dialdehyde starch dihydrazone and its metal complexes

Central metal atom	Temperature range (°C)	Corresponding weight loss (%)	Minimum of the DTG peak (°C) ^a	tgα
None	21–150 180–230 230–270 270–310 310–400 21–400	6.2 17.0 9.0 9.8 13.7 57.3	100 210	–0.66 –0.23 –0.26 –0.14
Ca	21–150 180–230 230–270 270–310 310–400 21–400	3.8 16.5 9.2 10.1 13.4 54.1	100 214	–0.64 –0.23 –0.26 –0.14
Cd	21–150 180–230 230–270 270–310 310–400 21–400	3.7 14.7 9.3 9.2 11.6 50.4	100 209	–0.42 –0.23 –0.25 –0.11
Co(II)	21–150 180–230 230–270 270–310 310–400 21–400	4.1 15.0 10.3 9.7 13.0 54.4	100 207	–0.40 –0.26 –0.28 –0.14
Cu(II)	21–150 180–230 230–270 270–310 310–400 21–400	2.6 12.4 12.7 9.6 6.7 45.7	100 208	–0.30 –0.33 –0.16 –0.07
Fe(II)	21–150 180–230 230–270 270–310 310–400 21–400	3.2 15.2 9.8 9.9 13.7 55.3	100 213	–0.39 –0.24 –0.24 –0.15
Mg	21–150 180–230 230–270 270–310 310–400 21–400	4.6 16.5 9.3 9.7 13.6 55.2	100 213	–0.71 –0.24 –0.24 –0.14
Mn(II)	21–150 180–230 230–270 270–310 310–400 21–400	4.7 16.5 9.5 10.3 12.8 55.7	100 210	–0.52 –0.24 –0.26 –0.13
Ni(II)	21–150 180–230 230–270 270–310 310–400 21–400	3.6 15.3 11.1 9.2 13.1 54.1	100 205	–0.38 –0.29 –0.17 –0.14

(continued on next page)

Table 5 (continued)

Central metal atom	Temperature range (°C)	Corresponding weight loss (%)	Minimum of the DTG peak (°C) ^a	tgα
Pb(II)	21–150	6.2	100	
	180–230	13.6	202	–0.35
	230–270	9.1		–0.23
	270–310	9.4		–0.23
	310–400	12.1		–0.11
	21–400	53.0		
Zn	21–150	2.4	100	
	180–230	15.4	213	–0.51
	230–270	10.2		–0.25
	270–310	10.3		–0.27
	310–400	13.1		–0.14
	21–400	53.1		

^a The main peaks.

tg α for this step was around –0.5 for the Mn(II) and Zn complexes, around –0.4 for Cd, Co(II), Fe(III), and Ni(II) complexes and around –0.3 for Cu(II) and Pb(II) complexes. There was a qualitative link between the level of the weight loss and the rate of that process. The rates of decomposition in the subsequent stage was generally lower, tgα in the majority of complexes was around –0.25. The further stage was insignificantly faster (tgα = –0.26). The fourth stage was significantly slower (tgα = –0.14). Similar rate and weight losses were recorded for the non-coordinated ligand. Thus, formation of metal complexes by intermediary dextrans and further products of their decomposition as well catalytic effect of metal ions on the decomposition was negligible.

4. Conclusions

1. It was shown that dialdehyde starch dihydrazone coordinated such metal ions as Ca, Cd, Co(II), Cu(II), Fe(II), Mg, Mn(II), Ni(II), Pb(II), and Zn. Degree of saturation of the ligand with metal ions was different for particular central metal atoms. Therefore, this compound can be considered as heavy metal ion trap.
2. The C=N and C–O–C groups were sites of coordination. The complexes had a distorted tetrahedral geometry.
3. The thermal decomposition of free and coordinated ligand proceeded in four steps. The coordination usually stabilized thermally the ligand. Except the complex with Mg, the rates of decomposition of the coordinated ligand were lower than that for free dialdehyde starch dihydrazone.

References

Sekkina, M. M., & Salem, M. R. (1997). Mechanism of thermal dehydrochlorination *o*-hydroxyacetophenone Girard-P hydrazone

- transition metal cation chloride complexes. *Journal of Thermal Analysis*, 48, 841–849.
- Agarwal, S. K., Jain, J., & Chand, S. (2002). Synthetic and antimicrobial studies of hexacoordinated ternary complexes of Mn(II) and Cu(II). *Asian Journal of Chemistry*, 14(1), 489–492.
- Bobrański, B. (1956). Quantitative Analysis of Organic Compounds (in Polish). Warsaw: PWN, 75–81.
- Constable, E. C., Khan, F. K., Lewis, J., Liptrot, M. C., & Raithby, P. R. (1985). The preparation and coordination chemistry of 2,2,2'-terpyridine macrocycles. *Part 4*, 333–335.
- Cotton, F. A., & Wilkinson, G. (1962a). Advanced Inorganic Chemistry. New York: John Wiley and Sons, 508–511.
- Cotton, F. A., & Wilkinson, G. (1962b). Advanced Inorganic Chemistry. New York: John Wiley and Sons, 726.
- Cotton, F. A., & Wilkinson, G. (1972). Advanced Inorganic Chemistry. New York: John Wiley and Sons, 918.
- Giordano, T. J., Palenik, G. J., Palenik, R. C., & Sullivan, D. A. (1979). Pentagonal-bipyramidal complexes. Synthesis and characterization of aqua(nitrate)[2,6-diacetylpyridine bis(benzoyl hydrazone)]cobalt(II) nitrate and diaqua[2,6-diacetylpyridine bis(benzoyl hydrazone)]nickel(II) nitrate dihydrate. *Inorganic Chemistry*, 18, 2445–2450.
- Johnson, D. K., Murphy, T. B., Rose, N. J., Goodwin, W. H., & Pickart, L. (1982). Cytotoxic chelators and chelates. 1. Inhibition of DNA synthesis in cultured rodent and human cells by aroylhydrazones and by a copper(II) complex of salicylaldehyde benzoyl hydrazone. *Inorganica Chimica Acta*, 67, 159–165.
- Koh, L. L., Kon, O. L., Loh, K. W., Long, Y. C., Ranford, J. D., Tan, A. L. C., & Tjan, Y. Y. (1998). Complexes of salicylaldehyde acylhydrazones: Cytotoxicity, QSAR and crystal structure of the sterically hindered *t*-butyl dimmer. *Journal of Inorganic Biochemistry*, 72, 55–162.
- Latha, K. P., Vaidya, V. P., Keshavayya, J., & Vagdevi, H. M. (2001). Synthesis, characterization and biological studies of complexes of 2-acetylnaphtho[2, 1-b]furan hydrazone. *Journal of Indian Council of Chemists*, 18(1), 31–36.
- Li, C., Wang, L., Meng, X., & Zhao, H. (1999). Synthesis, characterization and antitumor activity of benzaldehyde nitrogen mustard picolinoyl hydrazone complexes. *Transition Metal Chemistry*, 24, 206–209.
- Lozos, G. P., Hoffman, B. M., SIM 14 Program, QCPE No. 265.
- Narang, K. K., Pardey, J. P., & Singh, V. P. (1994). Synthesis, characterization physicochemical studies of some copper(II) tetrathio-cyanato dithallate(I) complexes with hydrazides and hydrazones. *Polyhedron*, 13, 529–538.
- Nawar, N., & Hosny, N. M. (1999). Transition metal complexes of 2-acetylpyridine *o*-hydroxybenzoylhydrazone (APo-OHBH): Their preparation, characterisation and antimicrobial activity. *Chemical Pharmaceutical Bulletin*, 47(7), 944–949.
- Nawar, N., & Hosny, N. M. (2000). Synthesis, spectral and antimicrobial activity studies of *o*-aminoacetophenone *o*-hydroxybenzoylhydrazone complexes. *Transition Metal Chemistry*, 25, 1–8.
- Para, A., & Ropek, D. (2000). Starch dialdehyde derivatives as novel complexions protecting entomopathogenic nematodes from heavy metals. *Chemia i Inżynieria Ekologiczna*, 7(11), 1213–1220.
- Para, A., Karolczyk-Kostuch, S., Hajdon, T., & Tomasik, P. (2000). Dialdehyde starch of low degree of oxidation and its derivatives. *Polish Journal of Food and Nutrition Sciences*, 9/50, 7–12.
- Para, A., Klisiewicz-Pańszczyk, T., & Jurek, I. (2001). Synthesis and in vitro tuberculostatic activity of Co(II), Cu(II) and Ni(II) complexes of dialdehyde starch dithiosemicarbazone. *Acta Poloniae Pharmaceutica-Drug Research*, 58(5), 405–408.
- Radecka-Paryzek, W., & Gdaniec, M. (1997). The preparation, spectral and X-ray crystallographic characterization of 2,6-diacetylpyridinedihydrazone complex with lead(II) nitrate. *Polyhedron*, 16, 3681–3686.
- Rakha, T. H., Ibrahim, K. M., Abdallah, A. M., & Hassanian, M. M. (1996). Synthesis and characterization of bivalent metal complexes of pyrrole-2-carboxaldehyde aroylhydrazones. *Synthesis and Reactivity in Inorganic and Metal-Organic Chemistry*, 26, 1113–1123.

- Richter, M., Augustat, S., & Schierbaum, F. (1968). Ausgewählte Methoden der Stärkechemie. Leipzig: VEB Fachbuchverlag, 110–112.
- Ropek, D., & Para, A. (2002). The effect of heavy metal ions and their complexons upon the growth, sporulation and pathogenicity of the fungus *Verticillium lecanii*. *Journal of Invertebrate Pathology*, 79, 123–125.
- Saripinar, E., Güzel, Y., Patat, S., Yildirim, I., Akcamur, Y., & Dimoglo, A. S. (1996). Electron-topological investigation of the structure-antitubercular activity relationship of thiosemicarbazone derivatives. *Arzneimittel -Forschung (Drug Research)*, 46(II)(8), 824–828.
- Shakir, M., & Varkey, S. P. (1994). Synthesis and structural characterization of cobalt(II), nickel(II) and copper(II) complexes of 18-membered mixed-donor macrocycles. *Polyhedron*, 13, 791–797.
- Singh, N. K., Singh, D. K., & Singh, J. (2001). Synthesis, characterization and biological activity of the complexes of manganese(III), cobalt(III), nickel(II), copper(II) and zinc(II) with salicylaldehyde thiobenzhydrazone. *Indian Journal of Chemistry, Section A: Inorganic, Bioinorganic, Physical, Theoretical and Analytical Chemistry*, 40A(10), 1064–1069.
- Tsukamoto, Y., Sato, K., Tanaka, K., & Yanai, T. (1997). Synthesis of 5-deoxy-5-oxomilbemycin A(4) 5-hydrazone derivatives and their activity against *Tetranychus urticae*. *Bioscience Biotechnology and Biochemistry*, 61(2), 304–311.
- Von Wagner, W. H., & Winkelmann, E. (1972). Untersuchungen über die tuberkulostatische Wirksamkeit neuartiger Benzaldehyd- und Thiophen-aldehyd- Thiosemicarbazone in vitro und in vivo. *Arzneimittel -Forschung (Drug Research)*, 22(10), 1713–1716.
- Yang, Z. Y., Yang, R. D., Li, F. S., & Yu, K. B. (2000). Crystal structure and antitumor activity of some rare earth metal complexes with Schiff base. *Polyhedron*, 19(26-27), 2599–2604.